



# LUND UNIVERSITY

## Adjuncts to the Conventional 12-Lead ECG: Assessment of High-Frequency QRS Components and Additional Leads

Trägårdh, Elin

2007

[Link to publication](#)

*Citation for published version (APA):*

Trägårdh, E. (2007). *Adjuncts to the Conventional 12-Lead ECG: Assessment of High-Frequency QRS Components and Additional Leads*. [Doctoral Thesis (compilation), Clinical Physiology (Lund)]. Department of Clinical Physiology, Lund University.

*Total number of authors:*

1

### General rights

Unless other specific re-use rights are stated the following general rights apply:

Copyright and moral rights for the publications made accessible in the public portal are retained by the authors and/or other copyright owners and it is a condition of accessing publications that users recognise and abide by the legal requirements associated with these rights.

- Users may download and print one copy of any publication from the public portal for the purpose of private study or research.
- You may not further distribute the material or use it for any profit-making activity or commercial gain
- You may freely distribute the URL identifying the publication in the public portal

Read more about Creative commons licenses: <https://creativecommons.org/licenses/>

### Take down policy

If you believe that this document breaches copyright please contact us providing details, and we will remove access to the work immediately and investigate your claim.

LUND UNIVERSITY

PO Box 117  
221 00 Lund  
+46 46-222 00 00

Lund University, Faculty of Medicine Doctoral Dissertation Series 2007:22

**Adjuncts to the Conventional 12-Lead ECG**  
Assessment of High-Frequency QRS Components  
and Additional Leads

**ELIN TRÄGÅRDH, MD**



**LUND UNIVERSITY**

Doctoral Thesis

2007

Department of Clinical Physiology

Lund University, Sweden

**Faculty opponent**

Professor Paul Kligfield, Cornell University, New York, NY, USA

The public defense of this thesis will, with due permission from the Faculty of Medicine at Lund University, take place in Föreläsningssal 1, Lund University Hospital, on Monday, 5 February 2007, at 13.15.

ISSN 1652-8220

ISBN 91-85559-90-3

Department of Clinical Physiology, Lund University, 221 00 Lund, Sweden

Printed by: Tryckeriet i E-huset, Lund, Sweden

A full text electronic version of this thesis is available at

<http://theses.lub.lu.se/postgrad>

© 2007 Elin Trägårdh

[elin.tragardh@med.lu.se](mailto:elin.tragardh@med.lu.se)

To David



# Contents

List of Publications	7
Summary	9
Summary in Swedish/Sammanfattning på svenska	11
Abbreviations	13
<b>1 Introduction</b>	<b>15</b>
1.1 Cardiac diseases studied in the thesis	15
1.2 The development and use of the ECG	17
1.3 High-frequency ECG	23
1.4 Cardiac magnetic resonance imaging	31
<b>2 Aims of the Work</b>	<b>33</b>
<b>3 Materials and Methods</b>	<b>35</b>
3.1 Patient material	35
3.2 ECG acquisition and analysis	36
3.3 Cardiac magnetic resonance imaging	38
3.4 Statistical analysis	38
<b>4 Results and Comments</b>	<b>41</b>
4.1 HF-QRS in patients with IHD and in normal subjects	41
4.2 HF-QRS vs. standard ECG in the prediction of LVM	43

4.3 HF-QRS in patients with BBB	45
4.4 16-lead ECG vs. 24-lead ECG in the diagnosis of MI	47
4.5 Limitations of the studies	49
4.6 In summary	50
5 Major Conclusions	51
References	53
Acknowledgments	59
Papers I-IV	61

## List of publications

This thesis is based on the following publications, which are referenced in the text by their Roman numerals.

- I. Trägårdh E, Pahlm O, Wagner GS, Pettersson J. Reduced high-frequency QRS components in patients with ischemic heart disease compared with normal subjects. *J Electrocardiol* 2004;37:157-162.
- II. Trägårdh E, Arheden H, Pettersson J, Wagner GS, Pahlm O. Determination of the ability of high-frequency ECG to estimate left ventricular mass in humans, determined by magnetic resonance imaging. *Clin Physiol Funct Imaging* 2006;26:157-162.
- III. Trägårdh E, Pettersson J, Wagner GS, Pahlm O. Reduced high-frequency QRS components in electrocardiogram leads facing an area of the heart with intraventricular conduction delay due to bundle branch block. *J Electrocardiol* 2006;(epub ahead of print).
- IV. Trägårdh E, Claesson M, Wagner GS, Zhou S, Pahlm O. Detection of acute myocardial infarction using the 12-lead ECG plus inverted leads (24-lead ECG) versus the 16-lead ECG (with additional posterior and right-sided electrodes). Manuscript.





## Summary

The standard 12-lead electrocardiogram (ECG) is one of the most commonly used methods for diagnosing heart disease. Standard ECG is not always optimal, however, and new ECG methods can provide additional information. Analysis of high-frequency QRS components (HF-QRS) has been shown to increase the diagnostic performance of the ECG. Since the amplitudes of the HF-QRS are low compared with those visible in the standard ECG, analysis of HF-QRS requires a low noise level, a sampling rate of at least 1000 Hz, and multibeat signal averaging. Methods for analyzing HF-QRS have been developed in collaboration with the Department of Electrosience at the Faculty of Engineering, Lund University.

Another method for increasing the diagnostic performance of the ECG is to add electrodes to provide leads that “see” parts of the heart not covered by conventional leads. This could be particularly interesting in diagnosing conditions such as acute myocardial infarction (MI), for example, for which it is important to initiate reperfusion treatment as soon as possible.

The overall objectives of the thesis are to investigate whether analysis of HF-QRS has the ability to provide information not available from the standard ECG and to investigate whether information from additional ECG leads can improve the diagnosis of acute MI.

In Study I, patients with ischemic heart disease had significantly lower HF-QRS compared with normal individuals. There was substantial interindividual variability, however, which probably limits the clinical usefulness of this method. The study also showed that HF-QRS are not related to sex or age.

In Study II, we investigated whether the amplitude of HF-QRS correlates to the left ventricular mass. This has been shown to be the case in previous studies in rabbits. Our study, however, showed that analysis of HF-QRS is no better than analysis of standard 12-lead ECG for determination of left ventricular mass.

In Study III, patients with intraventricular conduction delay had lower HF-QRS in leads with a positive electrode facing the area of the heart with the conduction delay. In areas of the heart with normal conduction velocity, the amplitudes of HF-QRS were normal or almost normal. These findings support the theory that HF-QRS relate to the conduction velocity of the heart.

In Study IV, we investigated whether additional leads can improve the diagnosis of acute MI. The accuracy of the conventional 12-lead ECG is poor for finding acute MI when certain coronary arteries are involved. Conventional 12-lead ECG was compared with 16-lead ECG (12-lead ECG plus 4 additional electrodes) as well as with 24-lead ECG (12-lead ECG plus the inverted leads of these 12 leads). The sensitivity for detecting acute MI increased when using the 16-lead or 24-lead ECG compared with the 12-lead ECG. The specificity, however, decreased slightly. If the aim is to increase sensitivity for detecting MI, clinicians should be advised to use the 24-lead ECG, since no additional electrodes are required.

# Populärvetenskaplig sammanfattning

Vanligt viloelektrokardiogram (EKG) med 12 avledningar är ett av de mest använda redskapen för diagnostik av hjärtsjukdom. Tidigare forskning har visat att detta EKG ej är optimalt, men att nya EKG-metoder kan ge viktig tilläggsinformation. En metod som i flera tidigare studier visat sig innehålla diagnostisk potential är analys av de högfrekventa signalkomponenterna i EKG. Registrering av EKG för högfrekvensanalys ställer speciella krav på utrustningen. Ett krav är att man måste kunna mäta signalstyrkan i EKG minst 1000 gånger per sekund. Ett annat krav är att man måste kunna ta bort mycket brus ur signalen eftersom det högfrekventa innehållet har låg signalstyrka. Metoder för att analysera högfrekventa EKG-komponenter har utvecklats tillsammans med institutionen för elektrovetenskap vid Lunds tekniska högskola.

En annan metod för att finna mer diagnostisk information i ett EKG är att lägga till elektroder för att skapa nya avledningar, som ”ser” delar av hjärtat som inte täcks in av de konventionella. Detta skulle t.ex. vara kliniskt användbart vid diagnostik av akut hjärtinfarkt, då det är viktigt att rätt diagnos ställs så snabbt som möjligt för att kunna ge patienten rätt vård innan hjärtskadan blivit alltför utbredd.

Målsättningen för avhandlingen var att undersöka om analys av högfrekventa EKG-komponenter kan tillföra diagnostisk information som inte finns tillgänglig i standard-EKG, samt att undersöka om information i extra EKG-avledningar kan förbättra diagnostiken av akut hjärtinfarkt.

I delarbete I visades att patienter med kranskärslssjukdom hade signifikant lägre amplituder av högfrekventa EKG-komponenter än friska individer. Det kan dock vara svårt att använda denna information kliniskt, då spridningen i storleken på de högfrekventa EKG-komponenterna mellan patienterna var stor. Studien visade även att det inte finns något samband mellan kön eller ålder och de högfrekventa EKG-komponenternas storlek.

I delarbete II undersöktes om storleken på högfrekventa EKG-komponenter korrelerar med massan på vänster hjärtkammare, vilket har visat sig vara fallet i studier på kaniner. Vår studie visade dock att analys av högfrekventa EKG-komponenter inte är bättre än analys av vanligt 12-avlednings-EKG för att avgöra vänsterkammarmassan.

I delarbete III visades att retledningshinder i hjärtat ger lägre amplituder av högfrekventa EKG-komponenter i avledningar som har elektroder ovanför områden med förlångsammad retledningshastighet. I områden där retledningshastigheten är normal var de högfrekventa EKG-komponenterna normala eller i stort sett normala. Fynden stödjer teorin att storleken på de högfrekventa EKG-komponenterna påverkas av retledningshastigheten i hjärtat.

I delarbete IV undersöktes om extra avledningar kan förbättra diagnostiken av akut hjärtinfarkt. Tidigare studier har visat att EKG är dåligt på att hitta akuta hjärtinfarkter då vissa kranskärl är drabbade. EKG-fynden vid konventionellt 12-avlednings-EKG jämfördes med 16-avlednings-EKG (12-avlednings-EKG plus 2 extra elektroder till höger på bröstkorgen och 2 på ryggen) och 24-avlednings-EKG (12-avlednings-EKG plus invertering av dessa 12 avledningar). Vi fann att 24- och 16-avlednings-EKG hittade fler akuta hjärtinfarkter än 12-avlednings-EKG. Däremot ökade andelen ”falskt positiva” något. Om målet är att hitta fler hjärtinfarkter med hjälp av EKG bör man därför använda 24-avlednings-EKG eftersom inga extra elektroder krävs.

## Abbreviations

BBB – bundle branch block  
CABG – coronary artery bypass grafting  
CK-MB – creatine kinase-MB isoenzyme  
ECG – electrocardiogram/electrocardiography  
EKG – elektrokardiogram/elektrokardiografi  
HF-QRS – high-frequency QRS components  
IHD – ischemic heart disease  
LBBB – left bundle branch block  
LVM – left ventricular mass  
LVMi – left ventricular mass index  
MI – myocardial infarction  
MRI – magnetic resonance imaging  
mV – millivolt  
 $\mu$ V – microvolt  
PTCA – percutaneous transluminal coronary angioplasty  
RBBB – right bundle branch block  
RAZ – reduced amplitude zone  
RMS – root-mean-square  
STEMI – ST-segment elevation myocardial infarction  
TnT – Troponin T  
WCT – Wilson's central terminal



# Chapter 1

## Introduction

### 1.1 Cardiac diseases studied in the thesis

#### Ischemic heart disease

Ischemic heart disease (IHD) is the most common cause of death in the western world, causing about half of all deaths. In Sweden, about 150 000 patients per year present to the emergency department with suspected or verified IHD. Due to better treatment and better prophylaxis, the number of deaths due to IHD has decreased during recent decades.<sup>1</sup>

The term “ischemic” implies an oxygen deficit due to low blood flow in relation to the demand of the tissue. The most common cause of diminished coronary blood flow is atherosclerosis. Atherosclerotic changes in the vessels begin developing during adolescence and increase as a consequence of genetic predisposition as well as other risk factors. The result is the development of atherosclerotic plaques that protrude into the vessel lumen and either partially or completely block blood flow.<sup>2</sup> Cardiac pain, angina pectoris, will appear when the cardiac workload is too great in relation to the coronary flow.

The electrocardiogram (ECG) has been the most important tool for diagnosing IHD for many decades. ECG still plays a major role because it is readily available and inexpensive. Other, more expensive diagnostic methods include stress tests, myocardial scintigraphy, coronary angiography, echocardiography, and magnetic resonance imaging (MRI).

Several therapeutic alternatives are available for patients with IHD. In those with chronic, stable IHD, pharmacological therapy often is the first choice. In cases of unstable or advanced disease, coronary artery bypass grafting (CABG) or percutaneous transluminal coronary angioplasty (PTCA) often is performed.



## Acute myocardial infarction

Myocardial infarction (MI) is defined as myocardial cell death due to prolonged ischemia. When one of the coronary arteries is acutely blocked—for example, by a thrombus from a ruptured atherosclerotic plaque—blood flow ceases in the vessel beyond the occlusion.<sup>3</sup> Such occlusion is the most common cause of death in many parts of the world, usually resulting from mechanical failure of the ventricles or from ventricular tachycardia or fibrillation. The muscle cells that receive no blood flow cannot sustain cardiac muscle function and will survive by anaerobic metabolism only until the glycogen reserve is depleted, unless blood flow is restored either by collateral vessels or by removal of the occluding thrombus. Infarcted muscle tissue is gradually replaced by fibrous tissue.

In the past, the discharge diagnosis of MI was determined by a combination of two of three characteristics: typical symptoms (i.e., chest discomfort), cardiac enzyme elevations, and typical ECG patterns involving the development of Q waves. Current clinical practice requires a more precise definition, however, especially for early detection of acute MI. Further, serological biomarkers and imaging techniques have improved, and the latter technology can identify patients with small areas of myocardial necrosis.<sup>4</sup> The preferred biomarker for detection of myocardial damage is cardiac troponin (I or T), which has nearly absolute myocardial tissue specificity as well as high sensitivity.<sup>5</sup> If cardiac troponin assays are not available, the best alternative is creatine kinase-MB isoenzyme (CK-MB). Troponin T (TnT) is a protein found both bound to the tropomyosin complex and in the cytosol, whereas CK-MB is a cytosolic protein; both are released when the membrane of the cardiac myocyte ruptures.

Today, one of two criteria establishes the diagnosis of acute, evolving, or recent MI. The first is a typical rise and gradual fall (troponin) or more rapid rise and fall (CK-MB) in biochemical markers with at least one of the following: a) ischemic symptoms, b) development of pathological Q waves on the ECG, c) ECG changes indicative of ischemia (ST-segment elevation or depression), or d) coronary artery intervention. The second criterion is post-mortem findings of acute MI.<sup>5</sup>

Prevention of infarction due to coronary occlusion is an important therapeutic aim. This can be done either by the use of thrombolytic drugs, in which the fibrinolytic system is stimulated to dissolve the occluding thrombus, or by mechanical restoration of the blood flow by PTCA or CABG. During PTCA,

a balloon is inflated at the location of the occlusion, followed by implantation of an expanded stent, and the artery is dilated. The use of CABG in patients with ongoing acute MI is limited to patients not suitable for PTCA. Other drugs also help reduce the damage from ischemia, including opioids (to prevent pain and reduce excessive sympathetic activity),  $\beta$ -adrenoceptor antagonists (to reduce cardiac work and thereby the metabolic needs of the heart), and glycoprotein IIb/IIIa inhibitors (to decrease aggregation of platelets and thereby increase the success of reperfusion efforts).

## **Left and right bundle branch block**

The heart has a specialized system for generating rhythmic impulses that cause contraction and for conducting these impulses rapidly through the heart muscle. The sinus node in the right atrium is normally the generator of the rhythmic impulses. The impulse spreads through the atria to the atrioventricular node and the His bundle, which conducts the impulse into the right and left bundle branches, which then conduct the impulse to different parts of the ventricles.

A bundle branch block (BBB) implies that impulse propagation is blocked in one of the bundles. The ventricle cannot be depolarized via the blocked bundle branch, so the impulse must reach it via the septal myocardium, which makes the conduction velocity lower. In a patient with left BBB (LBBB), the left ventricle cannot be depolarized via the left bundle branch, whereas the right ventricle is depolarized in a normal way. In a patient with right BBB (RBBB), the right ventricle cannot be depolarized normally. A BBB does not give rise to any symptoms, but it might indicate heart disease. LBBB is nearly always due to heart disease, most commonly fibrosis, whereas RBBB can occur in healthy individuals.<sup>6</sup> When LBBB is present, further analysis of the ECG for detection of acute coronary ischemia or left ventricular hypertrophy is almost impossible.

## **1.2 The development and use of the ECG**

The first ECG in humans was recorded in 1887 by Waller,<sup>7</sup> but the leads that were first used for diagnostic ECG were the three bipolar limb leads introduced by Einthoven<sup>8</sup> in the beginning of the 20th century. In the earliest systems, the patient's arms and legs were inserted into jars of conducting

solution that were connected to a galvanometer. Thus it was possible to measure the differences in electrical potential between the two arms (lead I). It was also possible to measure potential differences between the right arm and the left leg (lead II) as well as between the left arm and the left leg (lead III). The sum of the potentials in lead I and III equals the potential in lead II ( $I + III = II$ ). Thus, given the amplitudes in any two standard limb leads at a certain time, the amplitude of the third lead can be calculated. Einthoven developed the clinical analysis of ECGs during the early 20th century, especially regarding arrhythmias. He was awarded the Nobel Prize in 1924 for his contributions to the development of electrocardiography.

In early 1930s, Wilson<sup>9,10</sup> introduced a “central terminal” (WCT). By connecting the electrodes on the limbs, he created a virtual reference point and was able to measure potential differences between this reference point and a single electrode. The new lead system allowed chest leads to be recorded by measuring the potential difference between the chest electrode and the WCT. In 1938, the chest leads were standardized by the Cardiac Society of Great Britain and Ireland in cooperation with the American Heart Association.<sup>11</sup> Later that same year, the electrode positions of leads V1–V6 were described as we know them today (Figure 1).<sup>12,13</sup> The standardization of placement of the chest leads was a committee decision, made with the specific intent of standardizing research. These leads, also called “the precordial leads,” record the cardiac activity in the horizontal plane. The precordial leads provide a panoramic view of the electrical activity progressing horizontally from the right ventricle to the left ventricle.

The WCT also enabled three other limb leads: VR, VL, and VF. These leads measure the potential difference between the right arm and the WCT, the left arm and the WCT, and the left foot and the WCT, respectively. The sum of the three leads at any given time is zero. These leads are generally of low voltage, however, and were replaced. In 1942, augmented limb leads were developed that measure the potential differences between one limb and the average of the potentials at the other limbs. For example, the difference in potential between the left arm and the average of the potentials at the right arm and left leg produced lead aVL. In similar fashion, the other two augmented limb leads, aVR and aVF, were designed.<sup>14</sup> The relationship between the three augmented leads is  $aVR + aVL = -aVF$ .

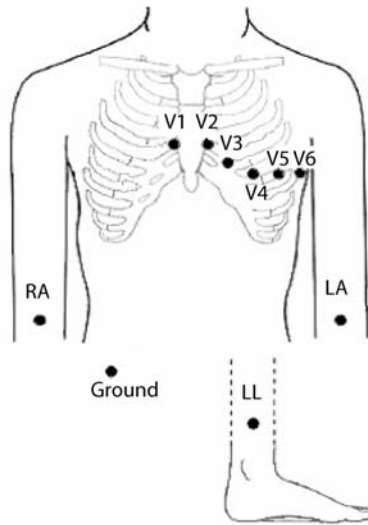


Figure 1. The electrode placement for the 12-lead ECG. RA = right arm, LA = left arm, LL = left leg.

The various leads described above (the original leads I, II, and III; the augmented additional leads aVR, aVL, and aVF; and the chest leads V1–V6) together form the lead system most commonly used today: the 12-lead ECG. In Sweden, it was decided to switch the polarity for lead aVR to minus aVR (–aVR), to present the limb leads as a contiguous panoramic sequence: aVL, I, –aVR, II, aVF, and III. This sequence represents “directions” in the frontal plane from  $-30^\circ$  to  $120^\circ$ , separated by intervals of  $30^\circ$ .

Figure 2 shows a normal ECG tracing from lead V5. The P wave represents the depolarization of the atria, the QRS complex represents the depolarization of the ventricles, and the T wave represents the repolarization of the ventricles. The repolarization of the atria occurs during the same time as the depolarization of the ventricles, and is usually hidden within the QRS complex.

During the last few decades, the use of computer-aided ECG recordings has become standard. Computerized acquisition and interpretation of ECGs was first accomplished in the 1960s and is today incorporated in almost all modern ECG-recording equipment.

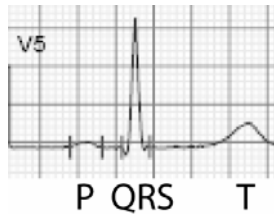


Figure 2. A normal ECG tracing from lead V5.

## Alternate lead systems

### Mason-Likar lead placement

When it is necessary to reduce noise from skeletal muscle (for example, during stress testing or analysis of high-frequency ECG), a different lead placement is used for the limb leads. In 1966, Mason and Likar<sup>15</sup> introduced a lead system with limb lead electrodes moved to the torso. The arm electrodes are placed in the left or right infraclavicular fossa, and the left leg electrode is placed in the anterior axillary line, between the costal margin and the crest of the ilium. The QRS morphology is slightly changed with this configuration compared with standard electrode placement. The amplitude of the R wave often increases in leads II, aVF, and III whereas it might decrease in leads aVL and I. Q waves due to inferior or posterior MI also may diminish or disappear compared with standard electrode placement.<sup>16,17</sup>

### Orthogonal lead system

The orthogonal lead systems are based on the principle that electric activity in the three-dimensional heart at one particular instant can be summed to one resultant vector. The most commonly used orthogonal lead system is that of Frank (1956).<sup>18</sup> The lead placement differs from that of the 12-lead ECG.

Frank leads are derived from seven electrodes: five on the chest, one on the neck, and one on the left foot. The three leads derived from the system are called X, Y, and Z, where X is similar to lead I or V6, Y is similar to lead II or aVF, and Z is similar to lead V2. It is possible to derive the X, Y, and Z leads from the 12-lead ECG, a synthesized vectorcardiogram.<sup>19</sup> Pairs of the orthogonal leads are combined to form loops (Figure 3). The collection of three loop projections is known as a vectorcardiogram. The appearance of the

loops can be used to diagnose various heart diseases, but this is not routinely used in clinical situations at present.

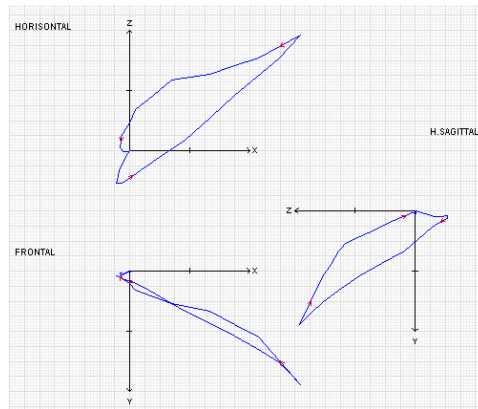


Figure 3. A vectorcardiogram from a patient with a normal 12-lead ECG. The three orthogonal leads X, Y, and Z are synthesized from the 12-lead ECG, and, from these leads, the QRS loops shown in the horizontal, frontal, and right sagittal planes are derived.

## Additional leads

The sensitivity of 12-lead ECG for detecting acute MI is known to be poor.<sup>20,21</sup> There are two principal reasons for this. First, the infarction might be too small to affect the electrophysiology detected by the ECG. Second, the location of the infarction might be in an area not covered by the 12-lead ECG. To increase the sensitivity to detect acute MI, additional chest electrodes can be placed all around the chest: leads V7–V9 on the back and leads V3R–V9R on the right side of the chest. These leads have been extensively studied for this use.<sup>22-29</sup>

Leads V7–V9 have been shown to detect posterior MI that is not detected by 12-lead ECG.<sup>22-25</sup> Thus sensitivity appears to be increased, but in some studies, specificity has been slightly decreased.<sup>26</sup> Right-sided chest leads have been found to have high sensitivity for detecting MI in the right ventricle.<sup>26-29</sup> Infarctions in this location are most often associated with inferior MI, and patients with inferior and right ventricular MI are known to have a poorer prognosis than patients with inferior MI alone.<sup>30-31</sup>

## 24-lead ECG

Instead of adding extra chest leads to improve the diagnostic ability of the ECG, it is possible to invert the existing leads in the same way that the Swedish standard already calls for the use of  $-aVR$  instead of  $+aVR$ . In this way, the chest leads plus the inverted chest leads produce a panoramic view of the transversal plane, and the limb leads plus the inverted leads give a panoramic view of the frontal plane (Figure 4).<sup>32</sup>

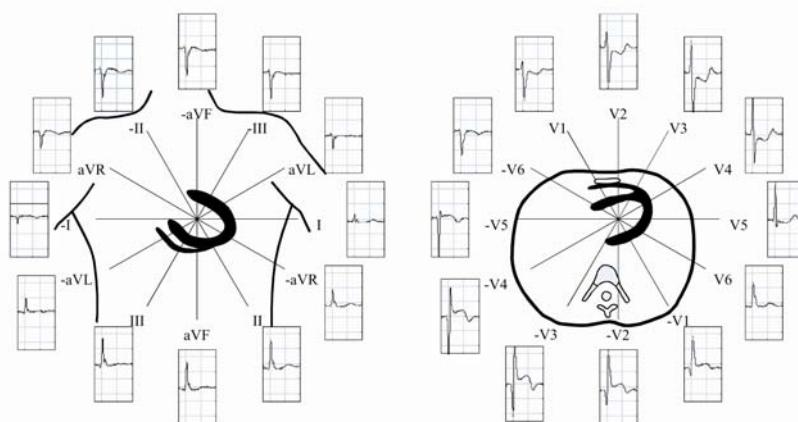


Figure 4. The 24-lead ECG. Note the ST-segment depression in leads V1–V4 and the ST-segment elevation in the corresponding negative leads. From reference [32] with permission.

The current ECG criteria for diagnosis of acute MI include only ST-segment elevation, and the term ST-segment elevation MI (STEMI) has been widely accepted. An acute posterior MI, however, is often represented by ST-segment depression in leads V1–V2.<sup>33</sup> Leads  $-V1$  and  $-V2$  would show ST-segment elevation in such cases, and thus it would be possible to diagnose STEMI without requiring changes in the current recommendations for ECG diagnosis. An alternative to inverting the leads from the 12-lead ECG would be simply to allow both ST-segment elevation and ST-segment depression to be diagnostic of acute MI. Ischemia that occurs during exercise testing often causes ST-segment depression, most commonly maximal in lead V5.<sup>34</sup> Therefore, the 24-lead ECG might have low specificity for detecting acute MI. A subset of the 24 leads might provide high sensitivity while retaining high specificity.

### 1.3 High-frequency ECG

The standard ECG is by convention limited to 0.05–150 Hz, but higher frequencies are also present in the ECG signal.<sup>35</sup> With high-resolution technology, it is possible to record and analyze these higher frequencies. The highest amplitudes of the high-frequency components are found within the QRS complex (Figure 5). In past years, the terms “high frequency”, “high fidelity”, and “wideband electrocardiography” have been used by several investigators to refer to the process of recording ECGs with an extended bandwidth of up to 1000 Hz. Several investigators have tried to analyze high-frequency QRS components (HF-QRS) in the hope that additional features seen in the QRS complex could provide information that would enhance the diagnostic value of the ECG.

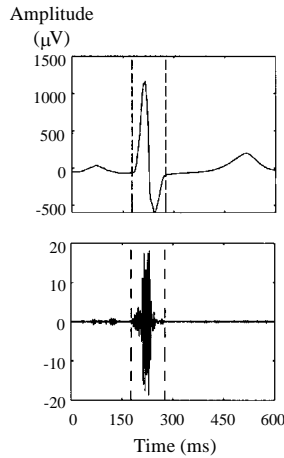


Figure 5. A signal-averaged ECG in the standard frequency range (upper panel) and the same signal-averaged ECG within the 150–250 Hz frequency range (lower panel). Dashed lines indicate the QRS duration. From reference [45] with permission.

The development of computerized ECG-recording devices that made it possible to record ECG signals with high resolution in both time and amplitude, as well as better possibilities to store and process the signals digitally, offered new methods for analysis. Several bandwidths and filter types have been applied for the extraction of HF-QRS as well as different signal-averaging techniques for noise reduction. There is no standard method for acquiring and quantifying HF-QRS.



The physiological mechanisms underlying HF-QRS are still not fully understood. One theory is that HF-QRS are related to the conduction velocity and the fragmentation of the depolarization wave in the myocardium. In a three-dimensional model of the ventricles with a fractal conduction system, high numbers of splitting branches were shown to be associated with more HF-QRS. This experiment also showed that the changes seen in HF-QRS in patients with myocardial ischemia might reflect slowing of the conduction velocity in the region of ischemia.<sup>36</sup> This mechanism has been tested by Watanabe et al.,<sup>37</sup> who infused sodium-channel blockers into the left anterior descending coronary artery in dogs. In their study, 60 unipolar ECGs were recorded from the entire ventricular surface and were signal-averaged and filtered in the 30–250 Hz frequency range. The decrease noted in the HF-QRS correlated linearly with the local conduction delay. The results suggest that HF-QRS are a potent indicator of disturbed local conduction. An alternative theory is that HF-QRS reflect the shape of the original electrocardiographic signal. Bennhagen et al.<sup>38</sup> showed that root mean square (RMS) values of the depolarization signal correlate poorly with the signal amplitude but correlate highly with the first and second derivatives, i.e., the velocity and the acceleration of the signal. The autonomic nervous system also might affect HF-QRS. For example, sitting upright causes significant change in HF-QRS in some leads compared with the supine position.<sup>39</sup> Unpublished results indicate that familial dysautonomic patients (both vagal and sympathetic degeneration) have very little reduced amplitude zone (RAZ) formation (see “Quantification of HF-QRS” below). Athletic individuals, especially elite athletes, who have vagally mediated changes on the conventional ECG (i.e., early repolarization, bradycardia) have increased RAZ formation (T Schlegel, personal communication). Further electrophysiological studies are needed, however, to better understand the underlying mechanisms of HF-QRS.

Several investigators have studied HF-QRS in different cardiac conditions, including acute myocardial ischemia and MI, but more knowledge is needed about the characteristics of HF-QRS before clinicians can use it as an adjunct to standard ECG.

## Analysis of HF-QRS

### ECG acquisition

To extract HF-QRS, it is important to use high resolution in both time and amplitude. In theory, the incoming ECG signal must be sampled (digitized) at a rate of at least twice that of the highest frequency of interest for the high-frequency signal retention; otherwise the signal will be distorted. This means that if the frequency range of interest is in the 150–250 Hz range, the sampling rate must be at least 500 Hz. In practice, a higher sampling rate is required, and in most studies on HF-QRS, the sampling rate has been 1000 Hz or more. Most modern ECG systems have an amplitude resolution of at least 1  $\mu\text{V}$ , which is enough for analysis of HF-QRS.

### Noise reduction

The amplitudes of HF-QRS are low ( $\mu\text{V}$ ) compared with the amplitudes seen in standard ECG (mV). To analyze HF-QRS, therefore, a low noise level is required. For example, skeletal muscles always contribute noise, which is typically in the high-frequency range. One way of reducing noise from skeletal muscles is to move the electrodes on the legs and arms to more proximal positions according to the Mason-Likar configuration.<sup>15</sup>

During clinical registration, signal averaging is necessary to obtain an acceptable signal-to-noise ratio. Thus the registration must sometimes continue for several minutes to obtain a large enough number of QRS complexes for averaging. If the ECG morphology is subject to dynamic changes—for example, during PTCA—an exponentially (recursively) updated beat average can be used instead, since blockwise averaging is not optimal in such cases.

During signal averaging, the mean amplitude is calculated at each instant of the cardiac cycle from many heartbeats. It is important to include values from exactly the same part of the cardiac cycle. To achieve this, a reference point (“fiducial point”) is identified, usually located close to the peak of the R wave. It is equally important that only “normal” beats are included in the average. Before signal averaging, the predominant beat morphology is selected as a “template beat”. The similarities between the beats are expressed as a cross-correlation coefficient.<sup>40</sup> Only beats with a correlation coefficient exceeding 0.97 are usually used for averaging. Signal averaging is continued until the noise is less than a certain level or until a certain number of beats has been included.

The signal averaging process is a well-known source of error during HF-QRS analysis. If the signal averaging is not done with high precision, HF-QRS in the calculated average will be affected. If a low cross-correlation coefficient is used, beats with different appearances will be lumped together. If the reference point is not reliable, the beats in the average will not be well aligned to one another (“trigger jitter”). These situations result in a reduction of the high-frequency content when averaging.

## Extraction of HF-QRS

HF-QRS are extracted from the signal-averaged beats through band-pass filtering. Often, a Butterworth filter is used.<sup>41</sup> This filter type has a nonlinear phase response, which can distort temporal relationships of the various signal components. Linear-phase filtering can be obtained, however, by first filtering the signal forward and then backward. Different studies have used different bandwidths when extracting HF-QRS. Most commonly, however, a frequency range between 150 and 250 Hz has been used.

## Quantification of HF-QRS

Several methods have been used for quantification of HF-QRS. One of the most common is to calculate RMS values during the entire QRS duration. This method quantifies the average amplitude of the signal and is calculated by:

$$\sqrt{\frac{\sum_{i=1}^n A_i^2}{n}}$$

where  $n$  is the number of measurements and  $A_i$ ,  $i = 1, \dots, n$ , are the measured amplitudes. To obtain an accurate RMS value, the beginning and end of the QRS complex must be identified correctly. The best delineation of the QRS complex is obtained when determining the QRS duration in the standard frequency range.

Another widely used method for quantification of HF-QRS is calculation of RAZs. The RAZ measure is a morphological measure, defined as an interval between two adjacent local maxima or two adjacent local minima in the HF-QRS, where a local maximum or minimum must have an absolute value higher than the three preceding and three following envelope points. The method was introduced by Abboud et al.<sup>42</sup> in the 1980s. It was discovered that areas with lower amplitude were present in the high-frequency signal in dogs with

myocardial ischemia but not in dogs with normal perfusion. The method has now been further developed by the National Aeronautics and Space Administration (NASA), and 3 different types of RAZs have been defined (Figure 6): “Abboud RAZ”, “Abboud-%-RAZ”, and “NASA RAZ” (most severe).<sup>43</sup> Other methods for quantification of HF-QRS include peak-to-peak amplitude and the integral of the signal.

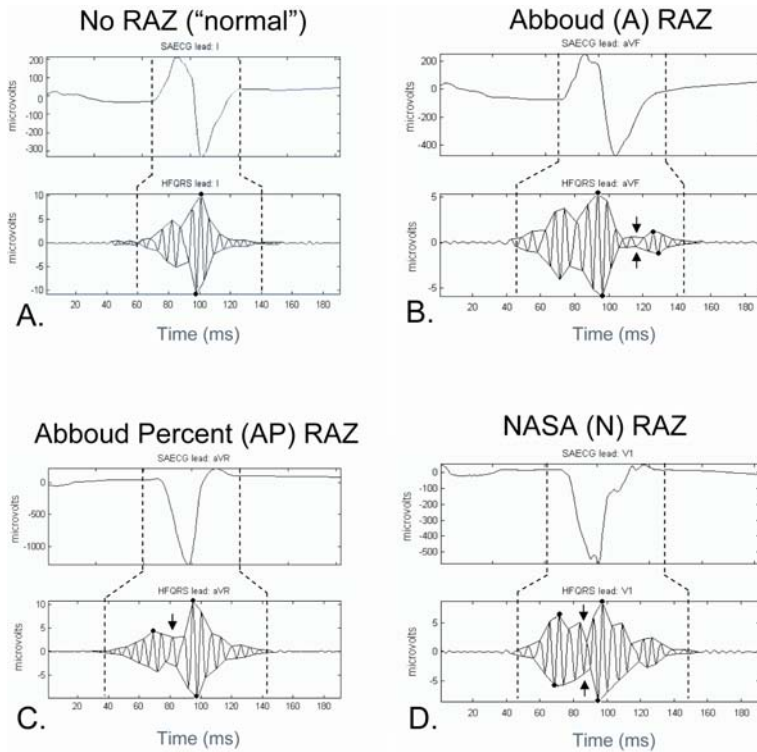


Figure 6. HF-QRS shown below the respective signal-averaged conventional ECG QRS complexes. Darkened circles in the HF-QRS denote local maxima and minima, whereas arrows (B-D) denote a RAZ. A, HF-QRS that contain no RAZs. B, HF-QRS that contain an Abboud RAZ on both the upper and lower portions of the signal. The amplitudes of both the secondary local maximum and minimum are insufficient to define an Abboud-% RAZ because they are less than 30% of the amplitudes of their corresponding primary local maximum and minimum. C, HF-QRS that contain an Abboud-% RAZ. D, HF-QRS that contain a NASA RAZ, because both a secondary local maximum and a minimum are present and both have amplitudes that are at least 30% of the amplitudes of their respective primary local maximum/minimum. From ref [43] with permission.

## Basic aspects of HF-QRS

The amplitude of HF-QRS differs among the 12 standard leads. The largest amplitudes are usually found in the anterior-posterior oriented leads (V2–V4) and in the inferior-superior oriented leads (II, aVF, and III). The lowest amplitudes are found in the left–right oriented leads (aVL, I, -aVR, V1, V5, and V6).<sup>44</sup> In the transverse plane, leads V1 and V6 are located farthest away from the left ventricle, possibly explaining the low amplitudes recorded in these leads. In the frontal plane, however, no leads are located close to the heart, but there is still a large difference in amplitude of HF-QRS among these leads.

The correlation between HF-QRS amplitudes and the QRS amplitudes in standard ECG is generally low. Factors beyond the QRS amplitude in standard ECG thus seem to influence the size of HF-QRS. There is also a large variation in HF-QRS between individuals. During consecutive registrations in the same individual, however, only small variations in HF-QRS are registered.<sup>44,45</sup>

## HF-QRS in acute myocardial ischemia

Several studies have reported lower HF-QRS amplitudes during acute myocardial ischemia. In a study in dogs, ECG was recorded both from epicardial electrodes and from surface electrodes during occlusion of the left anterior descending coronary artery. HF-QRS tracings recorded from the epicardium of the left ventricle were significantly reduced during the occlusion, whereas HF-QRS recorded from the nonischemic right ventricle remained unchanged. Reduced HF-QRS amplitudes were also noted from the surface electrodes.<sup>46</sup> Other animal studies have shown similar results.<sup>47-50</sup>

In humans, ECG tracings have been recorded during PTCA in two studies.<sup>51,52</sup> Ischemia led to changes in HF-QRS in a majority of the patients. These changes were observed even when no ST-segment changes in standard ECG were seen (Figure 7). Thus acute myocardial ischemia can be detected with higher sensitivity with analysis of HF-QRS compared with conventional analysis of standard ECG tracings. Analysis of HF-QRS might therefore serve as a complement to standard ECG in the detection of myocardial ischemia. The large interindividual variation in HF-QRS, however, probably makes high-frequency analysis most applicable to monitoring situations in which changes from baseline can be identified.

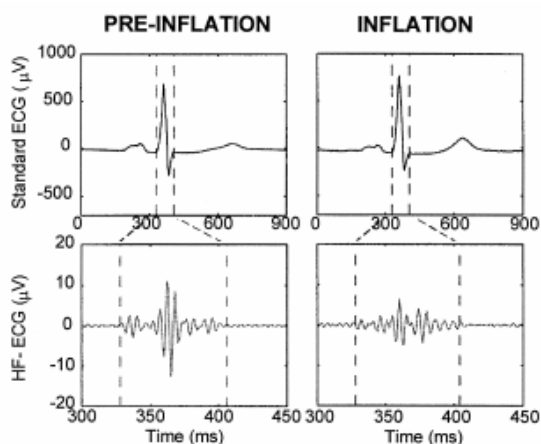


Figure 7. Signal-averaged ECGs before (left panels) and during PTCA balloon inflation (right panels) in the standard range (upper panel) and in the high-frequency range (lower panel) in lead V5. Dashed lines indicate the QRS duration. From reference [52] with permission.

During occlusion of the left anterior descending coronary artery, a reduction in HF-QRS is observed in many leads, most commonly in lead V3. During occlusion of other large coronary arteries, a reduction in HF-QRS is seen in various leads.<sup>52</sup> Thus, analysis of HF-QRS seems to be poorer than standard ECG in detecting the location of ischemia.

## HF-QRS in IHD

Several studies have compared HF-QRS in patients with old MI to HF-QRS in normal subjects. Most of these studies show a diminution of the amplitudes after old MI. In the frequency range of 80–300 Hz, HF-QRS are significantly lower in leads V2 and V5 in patients with old anterior MI compared with normal controls.<sup>53</sup> In patients with old inferior infarction, HF-QRS are reduced in leads II, aVF, and III.<sup>53,54</sup> When recording with Frank leads (X, Y, and Z leads), reduced HF-QRS are found in patients with old anterior and/or inferior infarction.<sup>55</sup> Some studies, however, have shown higher HF-QRS in patients with old MI compared with normal individuals, measured with frequencies >90 Hz using Frank leads.<sup>56</sup>

Studies of patients with angiographically documented IHD, with and without signs of old MI on ECG, have not shown any differences in HF-QRS between the two populations.<sup>57</sup>

When investigating serial changes in HF-QRS in the first year after acute MI, investigators have found a statistically significant increase in HF-QRS from a few days after the MI throughout the follow-up period.<sup>58</sup> The increase was small, however, and did not depend on MI location. Nor were there any differences in HF-QRS if reperfusion treatment had been received versus no treatment. Another study examined HF-QRS in patients with different MI locations and found no differences in HF-QRS in any lead between patients with anterior, inferior, or posterior MI.<sup>57</sup>

### **HF-QRS in stress-induced ischemia**

Analysis of HF-QRS during exercise testing has been suggested as a complement to assessment of the ST-segment changes for detection of exercise-induced ischemia. HF-QRS RMS voltages is known to increase during exercise in healthy individuals.<sup>59</sup> In a study comparing healthy individuals and patients with IHD, HF-QRS was significantly higher in the healthy population, both during and after exercise.<sup>60</sup> One problem with analysis of HF-QRS recorded during exercise is the high noise level generated by skeletal muscle.

A recent study investigated changes in both HF-QRS morphology and amplitude during adenosine myocardial perfusion imaging stress testing.<sup>61</sup> Analysis of HF-QRS was highly sensitive (94%) and specific (83%) for detecting reversible perfusion defects and significantly more sensitive (18%) than conventional ST-segment analysis. The best prediction of myocardial perfusion imaging perfusion defects was found to be a combination of RAZ measurements and changes in RMS values during the adenosine infusion.

### **HF-QRS in left ventricular hypertrophy**

Conventional ECG is one of the most common methods to detect left ventricular hypertrophy. Several different ECG-based criteria are used clinically. These methods, however, have low sensitivity at high levels of specificity. In a study in rabbits with and without left ventricular hypertrophy, HF-QRS correlated well with left ventricular mass (LVM).<sup>62</sup> This study also assessed the vector magnitude from orthogonal leads ( $\sqrt{X^2 + Y^2 + Z^2}$ ) in different frequency ranges. High-pass filtering at 44 Hz showed the best

correlation between LVM and HF-QRS ( $r = 0.84$ ). A high correlation between LVM and HF-QRS was also found among the healthy rabbits.

### **HF-QRS in conduction abnormalities**

In dogs, HF-QRS are reduced during periods of slow conduction velocity in the heart.<sup>37</sup> When sodium channel blockers (lidocaine, disopyramide, flecainide) were infused in the left anterior descending coronary artery while simultaneously recording ECGs from the entire ventricular surface, HF-QRS were significantly lower in the areas affected by the sodium channel blockers. Thus HF-QRS appear to be a potent indicator of disturbed local conduction.

### **HF-QRS after heart transplantation and heart surgery**

Allograft rejection is a major cause of morbidity and mortality in patients who have undergone heart transplantation. There is no reliable method for detecting rejection except endomyocardial biopsy. Some studies have investigated whether HF-QRS could be used as a noninvasive marker of rejection.<sup>63,64</sup> These studies have shown somewhat diverging results, with both increases and decreases in HF-QRS at rejection reported.

In a study of patients who had had heart surgery, reductions in HF-QRS were found to correlate with the dysfunction of the heart.<sup>65</sup> Thus HF-QRS might be used as a noninvasive marker of myocardial dysfunction after heart surgery. One study investigated the change in HF-QRS during aortic clamping in children undergoing heart surgery.<sup>66</sup> In this study, the recovery time of the HF-QRS significantly correlated with cardioplegic arrest time during surgery.

## **1.4 Cardiac magnetic resonance imaging**

MRI is a noninvasive imaging technique that uses magnets and radio waves to obtain images of the body. Unlike conventional radiography, which makes use of ionizing radiation, MRI is based on the magnetic properties of atoms. For clinical imaging, hydrogen nuclei each consisting of a single proton are used to generate a signal from various tissues. A powerful magnet generates a magnetic field. In addition to this main magnet, there are also 3 additional, low-strength magnets, called gradient magnets. The main magnet immerses the patient in a



stable magnetic field, and the gradient magnets create a variable field. Radiofrequency coils are used to transmit and receive signals to and from the tissue of interest.

According to quantum physics, the hydrogen nucleus spins around its own axis. As the positively charged nucleus spins, it generates a small magnetic field. When the hydrogen nuclei are exposed to a strong external magnetic field, this spin will align with this external field. The spins rotate with a frequency proportional to the strength of the external magnetic field, the “Larmour frequency”.

If radio wave pulses that have a frequency corresponding to the Larmour frequency are transmitted towards the aligned hydrogen atoms in tissues, the atoms will absorb the energy required to make them spin in a different direction. Thus, the energy from the radio-frequency pulse forces them to spin at a particular frequency, in a particular direction different from that of the main magnetic field. When the radio-frequency pulse is turned off, the hydrogen protons begin to return to their natural alignment within the magnetic field and release their excess stored energy. As the hydrogen nuclei spins return to their alignment with the external magnetic field, a radio wave (echo) is emitted. This signal is received by a receiver coil and transferred to a computer, and an image is obtained after postprocessing of the signal.

To create a tomographic image from the MR signal, a gradient system introducing small variations of the magnetic field is used. The gradient system is used first to select the slices to be studied and then to create spatial encoding of the selected image slices.

MRI is considered the gold standard for estimation of left ventricular volumes, ejection fraction,<sup>67,68</sup> and mass,<sup>69</sup> as well as MI size.<sup>70</sup> Accurate measurements can be provided because of high spatial and temporal resolutions (Figure 8).

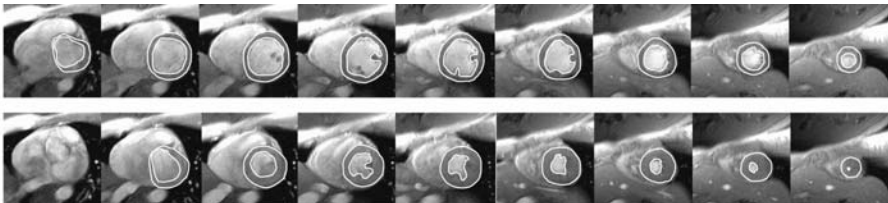


*Figure 8. Magnetic resonance short-axis images of the heart from base to apex (left to right) in diastole (upper row) and systole (lower row). The endo- and epicardial borders of the left ventricle are delineated.*

## Chapter 2

### **Aims of the work**

The general aim of this work was to gain knowledge about the characteristics of the ECG in high-frequency bands and its ability to detect heart disease, as well as to gain knowledge about the ability of additional ECG leads to detect acute MI.

The specific aim for each paper was to

- I. investigate the characteristics of HF-QRS in a normal population and compare HF-QRS in healthy individuals with those in patients with IHD.
- II. compare the ability of standard ECG and high-frequency ECG to predict LVM.
- III. test the hypothesis that HF-QRS are related to the conduction velocity of the heart by comparing patients who have LBBB or RBBB with those who have IHD and with normal individuals.
- IV. investigate whether additional ECG leads can detect acute MI better than standard 12-lead ECG, without a large decrease in specificity.



## Chapter 3

# Materials and methods

### 3.1 Patient material

Healthy individuals recruited by advertisement in Lund University Hospital, Lund, Sweden were used in Studies I, II, and III (n=62 or 63). All of these subjects had a normal resting ECG, were normotensive (blood pressure: <140 mm Hg systolic and <90 mm Hg diastolic), and had no direct or indirect signs of systemic or metabolic disease.

For Studies I and III, 64 patients with angiographically documented coronary artery disease were also studied. These patients were admitted for elective PTCA at the Charleston Area Medical Center, Charleston, WV, USA and had no chest pain or other symptoms suggestive of resting ischemia during the ECG recording.

Patients with LBBB (n=22) or RBBB (n=19) without any history of MI admitted to the Department of Clinical Physiology, Lund University Hospital, were also included for Study III.

For Study IV, 575 consecutive patients admitted to Lund University Hospital with acute chest pain were studied. Patients with a pacemaker, preexcitation, BBB, or left ventricular hypertrophy were excluded.

Approval was given by the local research ethics committees at Lund University and Charleston Area Medical Center. Informed consent was obtained from each subject before enrollment.

## 3.2 ECG acquisition and analysis

### ECG acquisition

The ECGs for Studies I–III were recorded using equipment from Siemens-Eléma AB, Solna, Sweden. Limb lead electrodes were placed using the Mason-Likar electrode configuration.<sup>15</sup> The chest leads were obtained using the standard electrode placement. The signals were digitized at a sampling rate of 1 kHz, with an amplitude resolution of 0.6  $\mu$ V. The ECG recordings were acquired continuously for 5 minutes, while the patient was resting in the supine position.

Using a 16-lead digital ECG recorder (HP XLi, Philips Medical Systems, Thousand Oaks, CA, USA), one 12-lead ECG plus leads V4R, V5R, V8, and V9 was recorded on each patient within 24 hours after admission for Study IV (postadmission ECGs). ECGs were recorded on patients in the cardiac catheterization laboratory, in the intermediate-care unit, and in the coronary-care unit. Digitally stored admission 12-lead ECGs obtained from routine clinical cases were also analyzed.

### Standard ECG analysis

The amplitudes (Study II) of the standard ECG were automatically determined in the obtained signal-averaged ECG. The measurements used to estimate LVM were the Cornell voltage measurement  $[R(aVL) + S(V3)]$ <sup>71</sup>, the Cornell product measurement (Cornell voltage \* QRS duration)<sup>71</sup>, and the Sokolow-Lyon measurement  $[S(V1) + R(V5/V6)]$ <sup>72</sup>. The peak-to-peak amplitude of the QRS complex was used as well.

The 12-lead ECG (Study IV) was regarded as indicative of acute MI if there was new or presumed new ST-segment elevation at the J point in two or more spatially contiguous leads, with thresholds of 0.2 mV in leads V1, V2, or V3 or 0.1 mV in other leads. Contiguity in the transverse plane was defined by the lead sequence V1–V6 and, in the frontal plane, by the lead sequence aVL, I, –aVR, II, aVF, and III.<sup>5</sup>

The 16-lead ECG was regarded as indicative of acute MI if the 12-lead ECG fulfilled the above criteria or if ST-segment elevation  $>0.05$  mV was present in at least one lead among V4R, V5R, V8, or V9 (based on observations in normal subjects).<sup>73</sup>

The 24-lead ECG was regarded as indicative of acute MI if there was new or presumed new ST-segment elevation at the J point in two or more spatially contiguous leads with cutoff points as given above for standard leads. The ST-segment elevation thresholds for the inverted leads were 0.05 mV in leads  $-V2$  and  $-V3$  and 0.1 mV in the other leads.<sup>74</sup>

## High-frequency ECG analysis

### Signal averaging

It is essential to reduce the noise level when analyzing the low-amplitude high-frequency signal. The technique used to reduce noise in this thesis was signal averaging. The predominant beat morphology was selected as “template beat”. The consecutive beats were then compared with the template beat. Similarities were expressed as “cross-correlation coefficient”. Only beats with a cross-correlation exceeding 0.97 were accepted for averaging (Studies I–III). The algorithm was developed by the Signal Processing Group, Department of Applied Electronics, Lund University, Sweden

### High-frequency QRS analysis

The HF-QRS in the signal-averaged ECGs were extracted with a third-order Butterworth filter<sup>40</sup> within a bandwidth of 150–250 Hz. Linear-phase filtering was obtained by first filtering the entire signal forward and then backward (so-called forward/backward filtering).

The determination of QRS onset and offset is a critical step, since errors affect the calculation of the RMS value. The QRS duration was automatically determined within the standard frequency range to reduce this type of error.<sup>75</sup> The average amplitude of the signal was calculated as RMS values:

$$\sqrt{\frac{\sum_{i=1}^n A_i^2}{n}}$$

where  $n$  is the number of measurements and  $A_i$ ,  $i = 1, \dots, n$ , are the measured amplitudes. An RMS value was calculated for each lead. The “total” HF-QRS was calculated as one value representing the sum of the RMS values of all leads. For Study II, “RMS-Sokolow-Lyon” was calculated by summing the RMS value in lead V1 and the highest RMS value in lead V5 or V6. Likewise,

the RMS values in leads aVL and V3 were summed (“RMS-Cornell voltage”) and “RMS-Cornell product” was calculated as QRS duration multiplied by RMS-Cornell voltage. These measurements were calculated in the 25–100, 50–150, and 150–250 Hz ranges.

The noise level was calculated in each lead and expressed as an RMS value during 100 ms, starting 100 ms after the QRS offset.

### **3.3 Cardiac magnetic resonance imaging**

MRI was performed on a 1.5-T system (Magnetom Vision, Siemens, Erlangen, Germany) with a 25-mT/m phased-array body coil. Subjects were placed in the supine position, and images were acquired while they held their breath. Short-axis cine images covering the entire left ventricle were acquired. Depending on heart size, 9–12 slices were required to completely cover the left ventricle. The image analysis was performed with publicly available software (Scion Image Beta 4.02, Scion Corporation, Frederick, MD, USA). The first frame of the cine image loop was selected as the end-diastolic image. The end-systolic image was chosen as the image containing the smallest left ventricular blood pool diameter. Endo- and epicardial borders were outlined manually on each end-diastolic and end-systolic image. To obtain the LVM, the planimetered area of each slice was multiplied by slice thickness.

### **3.4 Statistical analysis**

A multiple linear-regression model was used to test the associations between QRS duration, age, sex, and study group and HF-QRS (Study I). Differences in HF-QRS between patients with LBBB, RBBB, normal subjects, and patients with IHD were evaluated with one-way analysis of variance and Tukey’s post-hoc test (Study III). Due to lack of normality, the measurements were first logarithmically transformed (Studies I and III). For Study II, the Spearman rank-correlation coefficient was used to assess relationships between LVM/LVM index (LVMi) and ECG measurements. For Study IV, the sensitivity and specificity for MI were calculated for the 12-lead ECG, the 16-lead ECG, and the 24-lead ECG, using TnT/CK-MB as the gold standard.

The McNemar test was applied to examine differences in sensitivity and specificity between the sets of ECGs. Sensitivity and specificity were tested in pairs, that is, 12-lead ECG vs. 16-lead ECG, 12-lead ECG vs. 24-lead ECG, and 16-lead ECG vs. 24-lead ECG. For all studies, the level of significance was set at  $p < 0.05$ . Analyses were carried out using Minitab 13.30 (Minitab Inc., State College, PA, USA) (Study I) or SPSS 11.5 (SPSS Inc., Chicago, IL, USA) (Studies I–IV).





## Chapter 4

# Results and comments

### 4.1 HF-QRS in patients with IHD and in normal subjects (paper I)

In the normal study population, the mean HF-QRS varied from 2.0 to 4.9  $\mu\text{V}$  among the different leads. The mean of the summed HF-QRS for all patients was 43.7  $\mu\text{V}$  (range, 24.3–72.9). In patients with IHD, the mean RMS values varied between 1.7 and 4.1  $\mu\text{V}$  for the different leads. The mean summed HF-QRS was 33.5  $\mu\text{V}$  (range, 15.2–74.9). The pattern of amplitudes for the different leads was similar in both study groups, with the highest HF-QRS in the precordial leads V2–V4 and in the limb leads II, aVF, and III (Figure 9). A model was tested with a logarithmically transformed summed HF-QRS as the dependent variable and age, sex, QRS duration, and study population as independent variables. Age, sex, and QRS duration were not found to be significant ( $p=0.573$ ,  $p=0.820$ , and  $p=0.475$ , respectively), whereas study population was ( $p<0.0005$ ). Age, sex, and QRS duration were then excluded in a simple linear-regression model with log-summed HF-QRS as the dependent variable and study population as an independent variable. The  $p$ -value was  $<0.0005$  for this model.

Thus the study showed that the HF-QRS in patients with IHD is significantly lower than in normal subjects. It was further shown that HF-QRS do not seem to be associated with age, sex, or QRS duration. The interindividual variation was large, which probably restricts the clinical usefulness of the method.

The present study clarifies the controversial results from previous studies that evaluated HF-QRS in patients with old MI. Several investigators have reported reduced HF-QRS in patients with old MI compared with healthy subjects.<sup>53,76</sup> In contrast, Ringborn et al.<sup>57</sup> found no significant differences when

considering HF-QRS in patients with IHD, with or without old MI. The results of the present study and the previous studies indicate that HF-QRS are reduced in patients with IHD, regardless of the presence or absence of old MI.

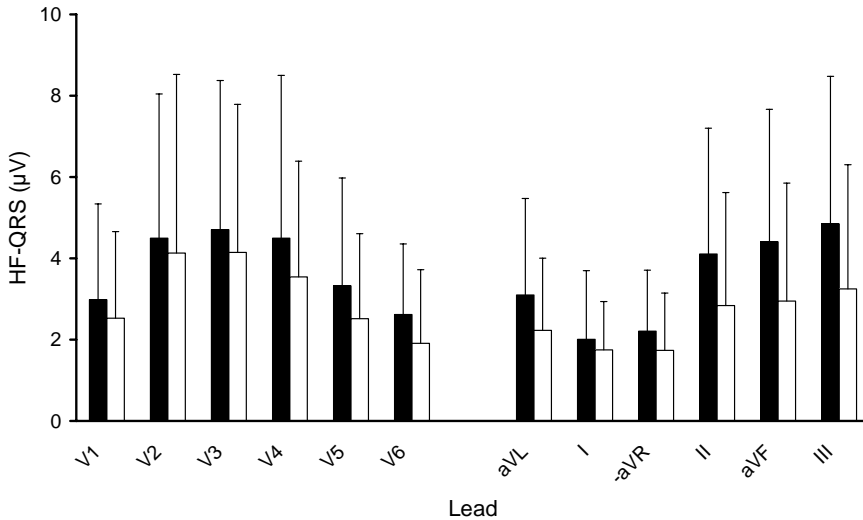


Figure 9. Mean HF-QRS ( $\mu V$ )  $\pm$  2 standard deviations in the 12 standard leads among normal subjects (black bars) and patients with IHD (white bars).

The physiological mechanisms underlying HF-QRS are not fully understood, but one theory is that HF-QRS relate to the conduction velocity of the myocardial cells and the conduction fibers. Several studies have shown that chronic IHD leads to structural changes in the myocardial tissue.<sup>77,78</sup> These morphological alterations include subendocardial proliferation of connective tissue, cellular swelling, and loss of myofibrillar content. The surface area of gap junctions also is reduced in chronically ischemic hearts.<sup>79</sup> This latter alteration might contribute to abnormal impulse propagation in the ischemic myocardium.<sup>79</sup> Abnormal propagation might be the reason for reduced HF-QRS in patients with IHD even in the absence of infarction.

## 4.2 HF-QRS vs. standard ECG in the prediction of LVM (paper II)

### LVM/LVMi vs. standard ECG QRS amplitudes

The correlation between LVM and Cornell voltage was  $\rho=0.31$ ; between LVM and Cornell product,  $\rho=0.40$ ; and between LVM and Sokolow-Lyon,  $\rho=0.35$ . The highest correlation between LVM and peak-to-peak amplitude was found in lead V3 ( $\rho=0.41$ ) (Figure 10). All correlations were found to be statistically significant.

The correlation was  $\rho=0.06$  between LVMi [LVM (g) divided by body weight (kg)] and Cornell voltage,  $\rho=0.08$  between LVMi and Cornell product, and  $\rho=0.30$  between LVMi and Sokolow-Lyon. The highest correlation between LVMi and peak-to-peak amplitude was found in lead aVL ( $\rho=0.36$ ) (Figure 11).

### LVM/LVMi vs. RMS values

In the 25–100 Hz frequency range, there was a significant correlation between LVM and RMS-Cornell product ( $\rho=0.35$ ), but not between LVM and any of the other variables (Figure 10). In the 50–150 Hz range, none of the correlations between LVM and RMS values was found to be statistically significant. In the 150–250 Hz range, the only significant correlation was between LVM and summed RMS ( $\rho=0.33$ ).

The best correlation between LVMi and RMS values in the 25-100 Hz range was found in lead V2 ( $\rho=0.33$ ). In this frequency band, the correlations in leads V1 and aVL as well as summed RMS were also found to be significant. In the 50–150 Hz range, the best correlation was found in lead V1 ( $\rho=0.37$ ) (Figure 11). Also significant were the correlations in leads V2 and V3, summed RMS, RMS-Sokolow-Lyon, RMS, Cornell voltage, and RMS-Cornell product. In the 150–250 Hz range, the only significant correlation was between LVMi and RMS-Cornell product ( $\rho=0.26$ ).

In rabbits, the high-frequency ECG has been shown to correlate better with LVMi than does the standard ECG, both when considering normal rabbits and animals with left ventricular hypertrophy ( $r=0.71$  in normal rabbits).<sup>62</sup>

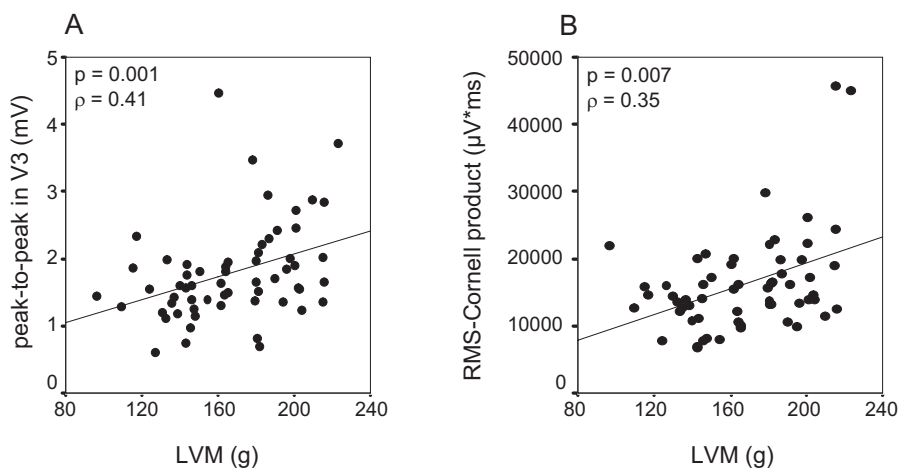


Figure 10. The best correlation between measurements based on standard ECG and LVM (A) and between HF-QRS measures and LVM (B). The best correlation between HF-QRS and LVM was found to be RMS-Cornell product in the 25–100 Hz range.

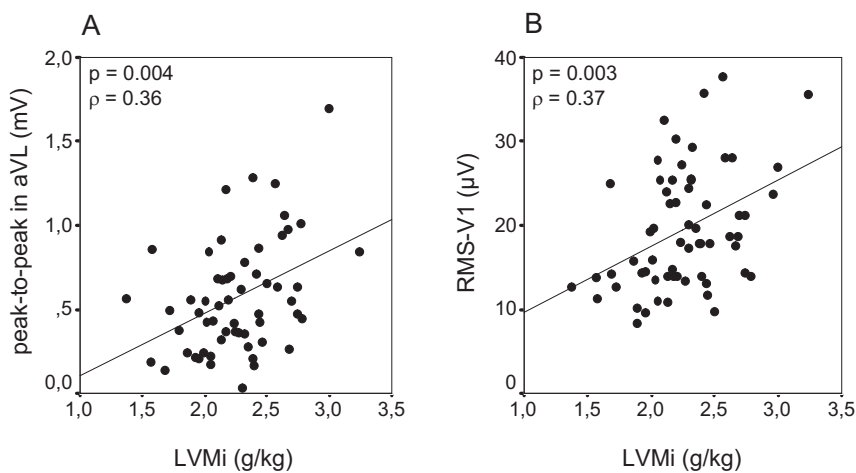


Figure 11. The best correlation between measurements based on standard ECG and LVMI (A) and between HF-QRS measures and LVMI (B). The best correlation between HF-QRS and LVMI was found to be RMS-V1 in the 50–150 Hz range.

The present study, however, shows similar results for standard ECG and HF-QRS, with a small advantage for the standard ECG. Thus standard ECG appears to be better suited for predicting LVM than are higher-frequency ranges. There is no obvious reason for the disparate findings in the present study versus that by Okin et al.<sup>62</sup>

For unknown reasons, a large interindividual variation in HF-QRS has been found in the 150–250 Hz range. This variation might hide any potential truly additional effects of LVM in this frequency range. However, HF-QRS have been shown to be quite reproducible within individuals,<sup>44,45</sup> which probably makes this method better for monitoring situations or when a previous recording is available.

### **4.3 HF-QRS in patients with BBB (paper III)**

The normal and IHD study populations used in this study for comparison with patients with LBBB or RBBB were the same as used in Study I. For HF-QRS results in these groups, please see p 41.

In patients with LBBB, the mean HF-QRS varied from 1.0 to 3.0  $\mu\text{V}$  among the different leads. The highest voltages were seen in leads V1–V3. The mean summed HF-QRS was 21.9  $\mu\text{V}$ . For RBBB patients, the mean HF-QRS varied between 1.9 and 3.7 among the leads. The highest voltages were seen in leads V2–V4, II, aVF, and III (Figure 12). The mean summed HF-QRS was 36.0  $\mu\text{V}$ .

When comparing patients with LBBB and normal subjects, HF-QRS in the LBBB group were significantly lower in all leads. Comparing LBBB patients with IHD patients, there was no statistically significant difference in HF-QRS in leads V1 and V2, but HF-QRS were lower in patients with LBBB in all other leads. When comparing patients with RBBB and normal subjects, only leads V1, aVL, and III showed a significant difference (higher in normal subjects). As for patients with IHD compared with normal subjects, the only leads that showed a statistically significant difference in HF-QRS were leads V5 and V6. Finally, when comparing LBBB patients and RBBB patients, HF-QRS were significantly higher in patients with RBBB in all leads except leads V1–V3, in which no differences were noted. The summed HF-QRS were significantly higher in normal subjects, patients with IHD, and patients with RBBB compared with the LBBB group.

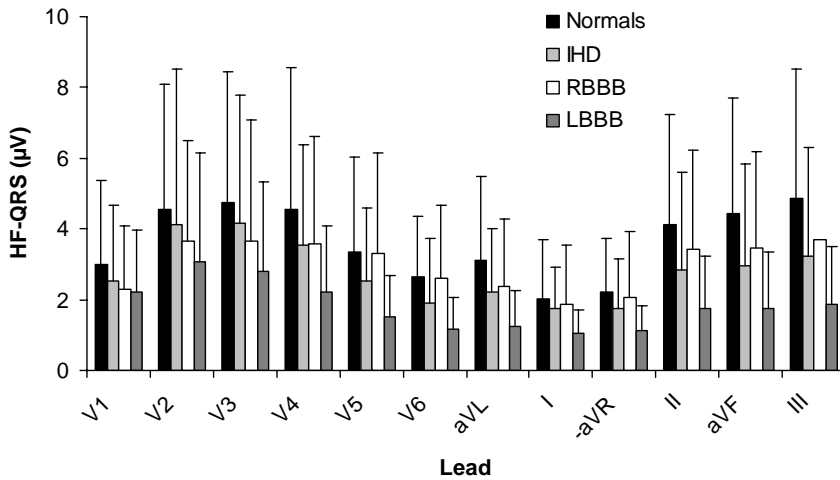


Figure 12. Mean HF-QRS ( $\mu V$ )  $\pm$  2 standard deviations in the 12 standard leads among normal subjects and patients with IHD, RBBB, or LBBB.

We found that HF-QRS in patients with LBBB were significantly lower than HF-QRS in normal subjects, in patients with IHD, and in patients with RBBB. This difference was smallest in leads V1 and V2 (not significant compared with the IHD group); that is, in leads close to the right ventricle, which is not affected by LBBB. We found few differences in HF-QRS in patients with RBBB compared with normal subjects or patients with IHD; among these were lead V1, a lead close to the right ventricle. HF-QRS are believed to be related to the conduction velocity of the heart. This has been simulated in a 3-dimensional heart model and by infusing sodium channel blockers into the left anterior descending coronary artery in dogs.<sup>36,37</sup> The latter study showed that the decrease noted in HF-QRS correlated linearly with the local conduction delay. The results of the present study support the hypothesis that HF-QRS are related to the conduction velocity.

## 4.4 24-lead ECG vs. 16-lead ECG in the diagnosis of MI (paper IV)

The study population consisted of 479 patients. Of these, 242 had acute MI and 237 had no acute MI according to biochemical markers.

Using the 12-lead ECG, the sensitivity for detecting acute MI was 28.1%. For the 16-lead ECG, the sensitivity was 33.1%, and for 24-lead ECG, 36.8%. The specificity for detecting acute MI was 97.0% for the 12-lead ECG, 93.2% for the 16-lead ECG, and 94.5% for the 24-lead ECG (Figure 13). There was a statistically significant difference in sensitivity between the 12-lead and 16-lead ECGs ( $p=0.013$ ) and between the 12-lead and 24-lead ECGs ( $p<0.001$ ), but not between the 16-lead and 24-lead ECGs ( $p=0.054$ ). For specificity, there was a statistically significant difference between the 12-lead and 16-lead ECGs ( $p=0.004$ ) and between the 12-lead and 24-lead ECGs ( $p=0.031$ ), but not between the 16-lead and 24-lead ECGs ( $p=0.581$ ).

The lead with maximum ST-segment elevation for patients with MI who showed MI on the 24-lead ECG but not on the 12-lead ECG was most often lead  $-V4$ . For the non-MI patients who showed MI on the 24-lead ECG but not on the 12-lead ECG, leads  $-V4$  and  $-V5$  most often had the maximum ST-segment elevation. For patients with or without MI who showed MI on the 16-lead ECG but not on the 12-lead ECG, lead  $V4R$  most often showed maximum ST-segment elevation.

In total, 43 patients with elevated biochemical markers did not receive acute MI treatment (thrombolysis or acute PTCA). Of these, four patients had ST-segment elevation on 12-lead ECG, but two were considered to have perimyocarditis (young men with a typical clinical course) and were excluded from the following analysis. The sensitivity for detecting acute MI among these 41 patients was 4.9% for the 12-lead ECG ( $n=2$ ), 17.1% for 16-lead ECG ( $n=7$ ), and 26.8% for the 24-lead ECG ( $n=11$ ). When regarding only the 14 patients with a CK-MB level  $>50$   $\mu\text{g/L}$ , the sensitivity for the 12-lead ECG was 7.1% ( $n=1$ ); for the 16-lead ECG, 14.3% ( $n=2$ ); and for the 24-lead ECG, 35.7% ( $n=5$ ). The 8 patients who had a CK-MB level  $>100$   $\mu\text{g/L}$  were further analyzed. The sensitivity for detecting MI among these patients was 0% for the 12-lead ECG, 12.5% for the 16-lead ECG ( $n=1$ ), and 37.5% for the 24-lead ECG ( $n=3$ ).

In a third analysis, digital admission ECGs (when available) were analyzed regarding 12-lead and 24-lead ECG. In all, 377 patients were included after



exclusions (the same exclusion criteria as above). A total of 166 patients had acute MI and 211 patients did not according to biochemical markers. The sensitivity for detecting acute MI was 32.5% for the 12-lead ECG and 48.8% for the 24-lead ECG. The difference was statistically significant ( $p < 0.001$ ). The specificity for the 12-lead ECG was 97.2%, and that for the 24-lead ECG, 93.8% (Figure 13). This difference also was statistically significant ( $p = 0.016$ ). The 24-lead ECG showed false-positive results for MI for 7 patients. Four of these patients showed maximum ST-segment elevation in lead  $-V_4$ , two in lead  $-V_3$ , and one in lead  $-V_6$ .

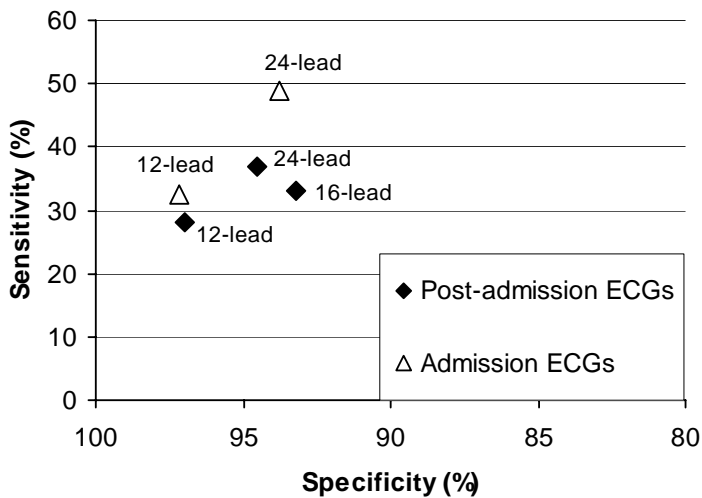


Figure 13. Receiver operating characteristic diagram of the sensitivity and specificity of the postadmission and admission ECGs.

The principal finding of this study was that the sensitivities of the 16-lead and 24-lead ECGs were significantly higher than the sensitivity of 12-lead ECG for detecting acute MI. There was no statistical difference in sensitivity between the 16-lead and 24-lead ECGs. Specificity, however, was significantly higher for the 12-lead ECG than for the 16- or 24-lead ECG. The sensitivity for diagnosing acute MI with the three ECG methods was very low overall, probably because most ECGs were recorded after treatment. In some cases the ST-segment elevation had already normalized. When regarding admission ECGs, the sensitivity increased by 16.3 percentage points when using the 24-

lead ECG compared with the 12-lead ECG, while the specificity decreased by 3.4 percentage points.

In patients with elevated biochemical markers who did not receive acute MI treatment, there was a much higher sensitivity for the 24-lead ECG than for the 12-lead ECG. Even when considering patients with larger infarctions (measured as CK-MB levels  $>50$  or  $>100$   $\mu\text{g/L}$ ), who could probably have benefited from acute thrombolysis or PTCA, more MIs were detected with the 24-lead ECG compared with 12-lead ECG. Thus some patients with acute MI detectable only by 24-lead ECG are perhaps being overlooked for acute treatment.

Of note, the leads with maximum ST-segment elevation in the 24-lead ECG in patients who did not have acute MI were  $-V4$  and  $-V5$  ( $-V4$  and  $-V6$  for admission ECGs). In a recent study, Perron et al. (A Perron, personal communication)<sup>80</sup> sequentially added inverted leads to the 12-lead ECG in patients who underwent prolonged PTCA, to identify a cutpoint at which the sensitivity to detect acute ischemia/infarction was significantly increased without a significant decrease in specificity. They concluded that a 19-lead ECG—leads  $-V1$ ,  $-V2$ ,  $-V3$ ,  $-aVL$ ,  $-I$ ,  $+aVR$ , and  $-III$  in addition to the standard 12 leads—had the highest sensitivity (78%) without a large decrease in specificity (to 93%). ST-segment depression in lead  $V5$  is known to have the highest sensitivity for detecting ischemia during exercise tests.<sup>34</sup> Thus some of the patients in the present study who had ST-segment elevation in leads  $-V4$ ,  $-V5$ , and  $-V6$ , but not elevated biochemical markers, might have had ischemia but not acute MI.

## 4.5 Limitations of the studies

In Studies I, II, and III normal individuals were included. This population was defined as subjects with normal resting ECG, normal blood pressure, no history of cardiac disease, and no signs of systemic or metabolic disease. Despite these inclusion criteria, there might have been subjects in the normal population who had IHD not noted on a resting ECG or reported by the individual.

Study II included only normal individuals. The range of LVM values might have been too small, and a better correlation might have been found if patients with left ventricular hypertrophy had been included.

In Study III, lack of information about the cardiac history of the patients with BBB is a limitation. Some of these patients could have had IHD, although patients with a history of MI were excluded. The patients were not matched for LVM and left ventricular function.

A major limitation of Study IV is that most postadmission ECGs were recorded after PTCA and thrombolytic medication, if any, would have been received. It would have been preferable to record all ECGs before treatment so as to observe higher sensitivities for the different ECG methods, but this was not logistically possible.

## **4.6 In summary**

The HF-QRS findings in the present study are not suitable for clinical use at present. However, more studies are needed before it is known whether HF-QRS can be a useful adjunct to the conventional 12-lead ECG.

The HF-QRS were significantly lower in patients with IHD compared with normal subjects, but interindividual differences were large. We learned, however, that there are electrophysiological differences between normal individuals and stable patients with IHD. We have also learned that HF-QRS are not predictive of LVM in normal individuals but might still be altered in patients with left ventricular hypertrophy. In Study III, HF-QRS were reduced in leads with a positive electrode facing the area with local conduction delay. Thus HF-QRS might reflect local effects more so than does standard ECG. In Study IV, there was a trend toward higher sensitivity for detecting MI with inversions of the standard 12 leads compared with a 16-lead ECG with “true” additional leads, thus giving better information about transmural ischemia than do posterior and right-sided electrodes.

## Chapter 5

### Major conclusions

The major conclusion of each paper was that:

1. The HF-QRS in patients with IHD were significantly lower than that in normal subjects. It may be difficult to use this information to discriminate clinically between normal subjects and patients with IHD, however, since interindividual variations were large. HF-QRS were not associated with age, sex, or QRS duration.
2. Contrary to previous results in animals, we found no better correlation between HF-QRS and LVM/LVMi than between standard ECG and LVM/LVMi in healthy human subjects.
3. The HF-QRS were lower in patients with LBBB compared with normal subjects and patients with IHD. The difference was small in leads V1 and V2. In patients with RBBB, few significant differences in HF-QRS could be detected; among these was lead V1. The results support the theory that HF-QRS are related to the conduction velocity of the heart.
4. The sensitivity of detecting acute MI was higher for the 16-lead and 24-lead ECGs than for the 12-lead ECG. Specificity, however, decreased slightly when using 24-lead and 16-lead ECGs. To increase the sensitivity for detecting MI, clinicians might wish to consider use of the 24-lead ECG or a subset thereof, since no additional electrodes are required beyond those of the conventional 12-lead ECG.



## References

1. Nordlander R, Schwan A. Ischemisk hjärtsjukdom. In: Läkemedelsboken 2003/2004. Uppsala: Almqvist & Wiksell Tryckeri AB, 2003.
2. Fallon JT. The pathophysiology of atherosclerosis of the coronary arteries and the changes that predispose to ischemic heart disease. In: Califf RM, Wagner GS, eds. *Acute Coronary Care*. Boston, MA: Martinus Nijhoff Publishing, 1985:33-39.
3. Naghavi M, Libby P, Falk E, et al. From vulnerable plaque to vulnerable patient: a call for new definitions and risk assessment strategies: Part I. *Circulation*. 2003;108:1664-1672.
4. Wagner A, Mahrholdt H, Holly TA, et al. Contrast-enhanced MRI and routine single photon emission computed tomography (SPECT) perfusion imaging for detection of subendocardial myocardial infarcts: an image study. *Lancet* 2003;361:374-379.
5. The Joint European Society of Cardiology/American College of Cardiology Committee. Myocardial infarction redefined – a consensus document of The Joint European Society of Cardiology/American College of Cardiology Committee for the Redefinition of Myocardial Infarction. *Eur Heart J* 2000;21:1502-1513.
6. De Pádua F, Pereirinha A, Lopes MG. Conduction defects. In: Macfarlane P, Lawrie T, eds. *Comprehensive Electrocardiology*. New York: Pergamon Press, 1989:459-509.
7. Waller A. A demonstration on man of electromotive changes accompanying the hearts beat. *J Physiol* 1887;8:229-234.
8. Einthoven W. The different forms of the human electrocardiogram and their signification. *Lancet* 1912;1:853-861 [reprinted in *Am Heart J* 1950;40:195-211].
9. Wilson F, MacLeod A, Barker P. The potential variations produced by the heart beat at the apices of Einthoven's triangle. *Am Heart J* 1931;7:207-211.
10. Wilson F, MacLeod A, Barker, et al. The electrocardiogram in myocardial infarction with particular reference to the initial deflections of the ventricular complex. *Heart* 1933;16:155-199.
11. Committee of the Cardiac Society of Great Britain and Ireland and Committee of the American Heart Association. Standardisation of precordial leads. *Lancet* 1938;221.
12. Barnes A, Pardee H, White P, et al. Standardization of precordial leads. *Am Heart J* 1938;15:107-108.
13. Barnes A, Pardee H, White P, et al. Standardization of precordial leads: supplementary report. *Am Heart J* 1938;15:235-239.

14. Goldberger E. A simple, indifferent, electrocardiographic electrode of zero potential and a technique of obtaining augmented, unipolar, extremity leads. *Am Heart J* 1942;23:483-492.
15. Mason RE, Likar I. A new system of multiple-lead exercise electrocardiography. *Am Heart J* 1966;71:196-205.
16. Papouchado M, Walker PR, James MA, et al. Fundamental differences between the standard 12-lead electrocardiography and the modified (Mason-Likar) exercise lead system. *Eur Heart J* 1987;8:725-733.
17. Sevilla DC, Dohrmann ML, Somelofski CA, et al. Invalidation of the resting electrocardiogram obtained via exercise electrode sites as a standard 12-lead recording. *Am J Cardiol* 1989;63:35-39.
18. Frank E. An accurate, clinically practical system for spatial vectorcardiography. *Circulation* 1954;13:737-749.
19. Macfarlane PW, Edenbrandt L, Pahlm O. 12-Lead Vectorcardiography. Oxford: Butterworth-Heinemann Ltd., 1995.
20. Speake D, Terry P. Towards evidence based emergency medicine: best BETs from the Manchester Royal Infirmary. First ECG in chest pain. *Emerg Med J* 2001;18:61-62.
21. Blanke H, Cohen M, Schlueter GU, et al. Electrocardiographic and coronary arteriographic correlations during acute myocardial infarction. *Am J Cardiol* 1984;54:249-255.
22. Matetzky S, Freimark D, Feinberg MS, et al. Acute myocardial infarction with isolated ST-segment elevation in posterior chest leads V7-9: "hidden" ST-segment elevations revealing acute posterior infarction. *J Am Coll Cardiol* 1999;34:748-753.
23. Matetzky S, Freimark D, Chouraqui P, et al. Significance of ST segment elevations in posterior chest leads (V7 to V9) in patients with acute inferior myocardial infarction: application for thrombolytic therapy. *J Am Coll Cardiol* 1998;31:506-511.
24. Agarwal JB. Routine use of a 15-lead electrocardiogram for patients presenting to the emergency department with chest pain. *J Electrocardiol* 1998;31(Suppl):172-177.
25. Zalenski RJ, Cooke D, Rydman R, et al. Assessing the diagnostic value of an ECG containing leads V4R, V8, and V9: the 15-lead ECG. *Ann Emerg Med* 1993;22:786-793.
26. Zalenski RJ, Rydman RJ, Sloan EP, et al. Value of posterior and right ventricular leads in comparison to the standard 12-lead electrocardiogram in evaluation of ST-segment elevation in suspected acute myocardial infarction. *Am J Cardiol* 1997;79:1579-1585.

27. Croft CH, Nicod P, Corbett JR, et al. Detection of acute right ventricular infarction by right precordial electrocardiography. *Am J Cardiol* 1982;50:421-427.
28. Lopez-Sendon J, Coma-Canella I, Alcasena S, et al. Electrocardiographic findings in acute right ventricular infarction: sensitivity and specificity of electrocardiographic alterations in right precordial leads V4R, V3R, V1, V2, and V3. *J Am Coll Cardiol* 1985;6:1273-1279.
29. Morgera T, Alberti E, Silvestri F, et al. Right precordial ST and QRS changes in the diagnosis of right ventricular infarction. *Am Heart J* 1984;108:13-18.
30. Correale E, Battista R, Martone A, et al. Electrocardiographic patterns in acute inferior myocardial infarction with and without right ventricle involvement: classification, diagnostic and prognostic value, masking effects. *Clin Cardiol* 1999;22:37-44.
31. Andersen HR, Nielsen D, Lund O, et al. Prognostic significance of right ventricular infarction diagnosed by ST elevation in right chest leads V3R to V7R. *Int J Cardiol* 1989;23:349-356.
32. Pahlm-Webb U, Pahlm O, Sadanandan S, et al. A new method for using the direction of ST-segment deviation to localize the site of acute coronary occlusion: the 24-view standard electrocardiogram. *Am J Med* 2002;113:75-78.
33. Brady WJ, Acute posterior wall myocardial infarction: electrocardiographic manifestations. *Am J Emerg Med* 1998;16:409-413.
34. Viik J, Lehtinen, Turjanmaa V, et al. The effect of lead selection on traditional and heart rate-adjusted ST-segment analysis in the detection of coronary artery disease during exercise testing. *Am Heart J* 1997;134:488-494.
35. Golden DP Jr, Wolthuis RA, Hoffler GW. A spectral analysis of the normal resting electrocardiogram. *IEEE Trans Biomed Eng* 1973;20:366-372.
36. Abboud S, Berenfeld O, Sadeh D. Simulation of high-resolution QRS complex using a ventricular model with a fractal conduction system. Effects of ischemia on high-frequency QRS potentials. *Circ Res* 1991;68:1751-1760.
37. Watanabe T, Yamaki M, Tachibana H, et al. Decrease in the high-frequency QRS components depending on the local conduction delay. *Jpn Circ J* 1998;62:844-848.
38. Bennhagen RG, Sörnmo L, Pesonen E, et al. High-frequency components in ECG analysed in guinea-pig Langendorff preparations. *Clin Physiol* 2001;21:576-583.
39. Douglas PK, Batdorf NJ, Evans RT, et al. Temporal and postural variation of 12-lead high frequency QRS electrocardiographic signals in asymptomatic individuals. *J Electrocardiol* 2006;39:259-265.
40. Pahlm O, Sörnmo L. Data processing of exercise ECGs. *IEEE Trans Biomed Eng* 1987;34:158-165.



41. Proakis JG, Manolakis DG. Digital Signal Processing – Principles, Algorithms, and Applications. Upper Saddle River, NJ: Prentice-Hall, 1996.
42. Abboud S, Cohen RJ, Selwyn A, et al. Detection of transient myocardial ischemia by computer analysis of standard and signal-averaged high-frequency electrocardiograms in patients undergoing percutaneous transluminal coronary angioplasty. *Circulation* 1987;76:585-596.
43. Schlegel TT, Kulecz WB, De Palma IJ, et al. Real-time 12-lead high-frequency QRS electrocardiography for enhanced detection of myocardial ischemia and coronary artery disease. *Mayo Clin Proc* 2004;79:339-350.
44. Pettersson J, Carro E, Edenbrandt L, et al. Spatial, individual, and temporal variation of the high-frequency QRS amplitude in the 12 standard electrocardiographic leads. *Am Heart J* 2000;139:352-358.
45. Batdorf NJ, Feiveson AH, Schlegel TT. Month-to-month and year-to-year reproducibility of high frequency QRS ECG signals. *J Electrocardiol* 2004;37:289-296.
46. Mor-Avi V, Shargorodsky B, Abboud S, et al. Effects of coronary occlusion on high-frequency components of the epicardial electrogram and body surface electrocardiogram. *Circulation* 1987;76:237-243.
47. Abboud S. Subtle alterations in the high-frequency QRS potentials during myocardial ischemia in dogs. *Comput Biomed Res* 1987;20:384-395.
48. Abboud S, Smith JM, Shargorodsky B, et al. High frequency electrocardiography of three orthogonal leads in dogs during a coronary artery occlusion. *Pacing Clin Electrophysiol* 1989;12:574-581.
49. Abboud S, Cohen RJ, Sadeh D. A spectral analysis of the high frequency QRS potentials observed during acute myocardial ischemia in dogs. *Int J Cardiol* 1990;26:285-290.
50. Mor-Avi J, Akselrod S. Spectral analysis of canine epicardial electrogram; short term variations in the frequency content induced by myocardial ischemia. *Circ Res* 1990;66:1681-1691.
51. Pettersson J, Lander P, Pahlm O, et al. Electrocardiographic changes during prolonged coronary artery occlusion in man: comparison of standard and high-frequency recordings. *Clin Physiol* 1998;18:179-186.
52. Pettersson J, Pahlm O, Carro E, et al. Changes in high-frequency QRS components are more sensitive than ST-segment deviation for detecting acute coronary artery occlusion. *J Am Coll Cardiol* 2000;36:1827-1834.
53. Goldberger AL, Bhargava V, Froelicher V, et al. Effect of myocardial infarction on high-frequency QRS potentials. *Circulation* 1981;64:34-42.

54. Goldberger AL, Bhargava V, Froelicher V, et al. Effect of myocardial infarction on the peak amplitude of high frequency QRS potentials. *J Electrocardiol* 1980;13:367-372.
55. Berkalp B, Baykal E, Caglar N, et al. Analysis of high frequency QRS potentials observed during acute myocardial infarction. *Int J Cardiol* 1993;42:147-153.
56. Novak P, Zhixing L, Novak V, et al. Time-frequency mapping of the QRS complex in normal subjects and in postmyocardial infarction patients. *J Electrocardiol* 1994;27:49-60.
57. Ringborn M, Pahlm O, Wagner GS, et al. The absence of high-frequency QRS changes in the presence of standard electrocardiographic QRS changes of old myocardial infarction. *Am Heart J* 2001;36:1827-1834.
58. Trägårdh E, Pahlm O, Hedén B, et al. Serial changes in the high-frequency ECG during the first year following acute myocardial infarction. *Clin Physiol Funct Imaging* 2006;26:296-300.
59. Bhargava V, Goldberger AL. Effect of exercise in healthy men on QRS power spectrum. *Am J Physiol* 1982;243:H964-H969.
60. Beker A, Pinchas A, Erel J, et al. Analysis of high frequency QRS potential during exercise testing in patients with coronary artery disease and in healthy subjects. *Pacing Clin Electrophysiol* 1996;19:2040-2050.
61. Rahman MA, Gedevarishvili A, Birnbaum Y, et al. High-frequency QRS electrocardiogram predicts perfusion defects during myocardial perfusion imaging. *J Electrocardiol* 2006;39:73-81.
62. Okin PM, Donnelly TM, Parker TS, et al. High-frequency analysis of the signal-averaged ECG. Correlation with left ventricular mass in rabbits. *J Electrocardiol* 1992;25:111-118.
63. Valentino VA, Ventura HO, Abi-Samra FM, et al. The signal-averaged electrocardiogram in cardiac transplantation. A non-invasive marker of acute allograft rejection. *Transplantation* 1992;53:124-127.
64. Graceffo MA, O'Rourke RA. Cardiac transplant rejection is associated with a decrease in the high-frequency components of the high-resolution, signal-averaged electrocardiogram. *Am Heart J* 1996;132:820-826.
65. Matsushita S, Sakakibara Y, Imazuru T, et al. High-frequency QRS potentials as a marker of myocardial dysfunction after cardiac surgery. *Ann Thorac Surg* 2004;77:1293-1297.
66. Abe M, Matsushita S, Mitsui T. Recovery of high-frequency QRS potentials following cardioplegic arrest in pediatric cardiac surgery. *Pediatr Cardiol* 2001;22:315-320.

67. Bellenger N, Davies L, Francis J, et al. Reduction in sample size for studies of remodeling in heart failure by the use of cardiovascular magnetic resonance. *J Cardiovasc Magn Reson* 2000;2:271-278.
68. Lorenz C, Walker E, Morgan V, et al. Normal human right and left ventricular mass, systolic function, and gender differences by cine magnetic resonance imaging. *J Cardiovasc Magn Reson* 1999;1:7-12.
69. Bottini P, Carr A, Prisant L, et al. Magnetic resonance imaging compared to echocardiography to assess left ventricular mass in the hypertensive patient. *Am J Hypertens* 1995;8:221-218.
70. Kim R, Fieno D, Parrish T, et al. Relationship of MRI delayed contrast enhancement to irreversible injury, infarct age, and contractile function. *Circulation* 1999;100:1992-2002.
71. Molloy TJ, Okin PM, Devereux RB, et al. Electrocardiographic detection of left ventricular hypertrophy by the simple QRS duration-voltage product. *J Am Coll Cardiol* 1992;20:1180-1186.
72. Sokolow M, Lyon TP. Ventricular complex in left ventricular hypertrophy as obtained by unipolar precordial and limb lead. *Am Heart J* 1949;37:161-186.
73. Andersen HR, Nielsen D, Gadegaard LH. The normal right chest electrocardiogram. *J Electrocardiol* 1987;20:27-32
74. Macfarlane P. Appendix 1: Normal limits. In : Macfarlane P, Lawrie T, eds. *Comprehensive Electrocardiology*. New York: Pergamon Press, 1989:1442-1525.
75. Jonson B, Lundh B, Pahlm O, et al. Determination of QRS onset and end in orthogonal and scalar ECGs. A new approach. *Comput Cardiol* 1984;459-462.
76. Bhargava V, Goldberger A. Myocardial infarction diminishes both low and high frequency QRS potentials: power spectrum analysis of lead II. *J Electrocardiol* 1981;14:57-60.
77. Katagiri T, Toba K, Takeyama Y, et al. Morphologic and biochemical studies on the experimental chronic ischemic myocardium with the Ameroid constrictor. *Jpn Circ J* 1978;42:345-352.
78. Vanoverschelde JL, Wijns W, Depre C, et al. Mechanisms of chronic regional postischemic dysfunction in humans. New insights from the study of noninfarcted collateral-dependent myocardium. *Circulation* 1993;87:1513-1523.
79. Peters NS, Green CR, Poole-Wilson PA, et al. Reduced content of connexin43 gap junctions in ventricular myocardium from hypertrophied and ischemic human hearts. *Circulation* 1993;88:864-875.
80. Wagner GS, Pahlm O, Selvester R. Consideration of the 24-lead electrocardiogram to provide ST-elevation myocardial infarction equivalent criteria for acute coronary occlusion. *J Electrocardiol* 2006;39:S62-S67.

# Acknowledgments

Many people have helped and encouraged me on my way in this work, for which I am most grateful. I would especially like to thank:

**Olle Pahlm**, my supervisor, for being the supervisor every PhD student wishes for.

**Jonas Pettersson**, my co-supervisor, for introducing me to the field of HF-QRS.

**Galen Wagner**, my co-supervisor, for many interesting and rewarding discussions.

**Leif Sörnmo** for helping me in the field of signal processing.

**Håkan Arheden** for encouragement and for providing many interesting aspects of leadership and life in general.

**Björn Jonson** for providing insight into the academic world.

**Annika Welinder**, **Eva Persson**, **Michael Ringborn**, and **Bo Hedén** for support and great friendship, especially during travels.

**Henrik Engblom** for helping me with MRI.

My co-authors **Sophia Zhou** and **Mikaela Claesson** for your contributions.

**Kerstin Brauer** for help with graphics.

**Todd** and **Maya Schlegel** and **Brian Arenare** for your great hospitality in Houston and for being fun and inspiring research partners.

**Ulf Ekelund** and **Johan Brandt** for providing me with valuable directions at the halftime examination.

**Kristoffer Peters**, **Per-Erik Isberg**, **Jan Lanke**, and **Jonas Björk** for statistical advice.

**Karin Larsson**, **Märta Granbohm**, **Kathy Shuping**, and **Beverly Perkins** for secretarial assistance.

Everybody at the **Department of Clinical Physiology** in Lund for introducing me to the clinical world and for helping me to find patients for the

studies. A special thank to **Bengt Jönsson** for your enthusiasm in recording study ECGs.

My parents **Gun** and **Christian** and my brother **Magnus** for love and support.

And finally, to **David**, for your love and for sharing life.

The studies in the thesis were supported by grants from the Swedish Heart Lung Foundation, the Faculty of Medicine at Lund University, the Region of Scania, and Philips Medical Systems.

## **Papers I-IV**

Published articles are reprinted with kind permission of the respective copyright holders.